Wind and Structures, Vol. 1, No. 4 (1998) 317-336
DOI: http://dx.doi.org/10.12989/was.1998.1.4.317

Appraisal of deployable dome structures under wind loading

G.A.R. Parke†, N. Toy‡ and E. Savory‡†

Department of Civil Engineering University of Surrey, Guildford, Surrey GU2 5XH, U.K.

K. Abedi‡‡ and R. Chenaghlou‡‡

Department of Engineering, Sahand University of Technology, Tabriz, Iran

Abstract. In this paper the appraisal of a folding dome structure under the influence of wind loading is discussed. The foldable structure considered is constructed from an assembly of interconnected elements, together with a flexible membrane, all of which are initially stored in a compact form and on deployment expand, like an umbrella, into a dome structure. Loading on the dome was obtained from a wind tunnel analysis of the pressure distribution over the roof of a 1:10 scale model of the structure. The critical loading obtained from the wind tunnel investigation was used, together with individual member and material tests, to form a series of numerical non-linear finite element models which were, in turn, used to investigate the forces within the structure. The numerical analysis was used to determine the critical wind loading that the structure can sustain, as well as providing a method by which to investigate the failure modes of the structure. In order to enhance the load carrying capacity of the dome it was found that both the strength and stiffnesss of the structural nodes needed to be enhanced and in addition, changes were necessary to substantially increase the stiffness of the individual member end caps.

Key words: folding dome; wind loading; structural analysis; structural collapse.

1. Introduction

The development of flexible membrane type structures has been very successful over the past twenty years and includes both the self-supporting type as well as the air-supported configuration (Lewis 1998). The latter usually derives its form, structural integrity, strength and stability from the pressure difference between the internal and external pressures across the membrane, with the internal pressure being supplied from an air generator. The former is dependent upon the form and topology of a light space frame for its strength, stability and appearance (Gantes *et al.* 1989).

The individual members forming part of a large span skeletal steel or aluminium alloy dome are usually designed according to British Standard 5950 Part 1 (1990) or British

† Reader
‡ Professor
‡† Lecturer
‡‡ Senior Lecturer

Standard 8118 Part 1 (1991), respectively, or a similar 'Code of Practice', depending on the country of origin. However, the same rigorous design approach is still normally applied to smaller span domes that are often used for recreational or even functional events. This class of structure is generally supposed to be suitable for use in moderate environmental conditions although they can also be set in adverse weather conditions. In this case these structures,

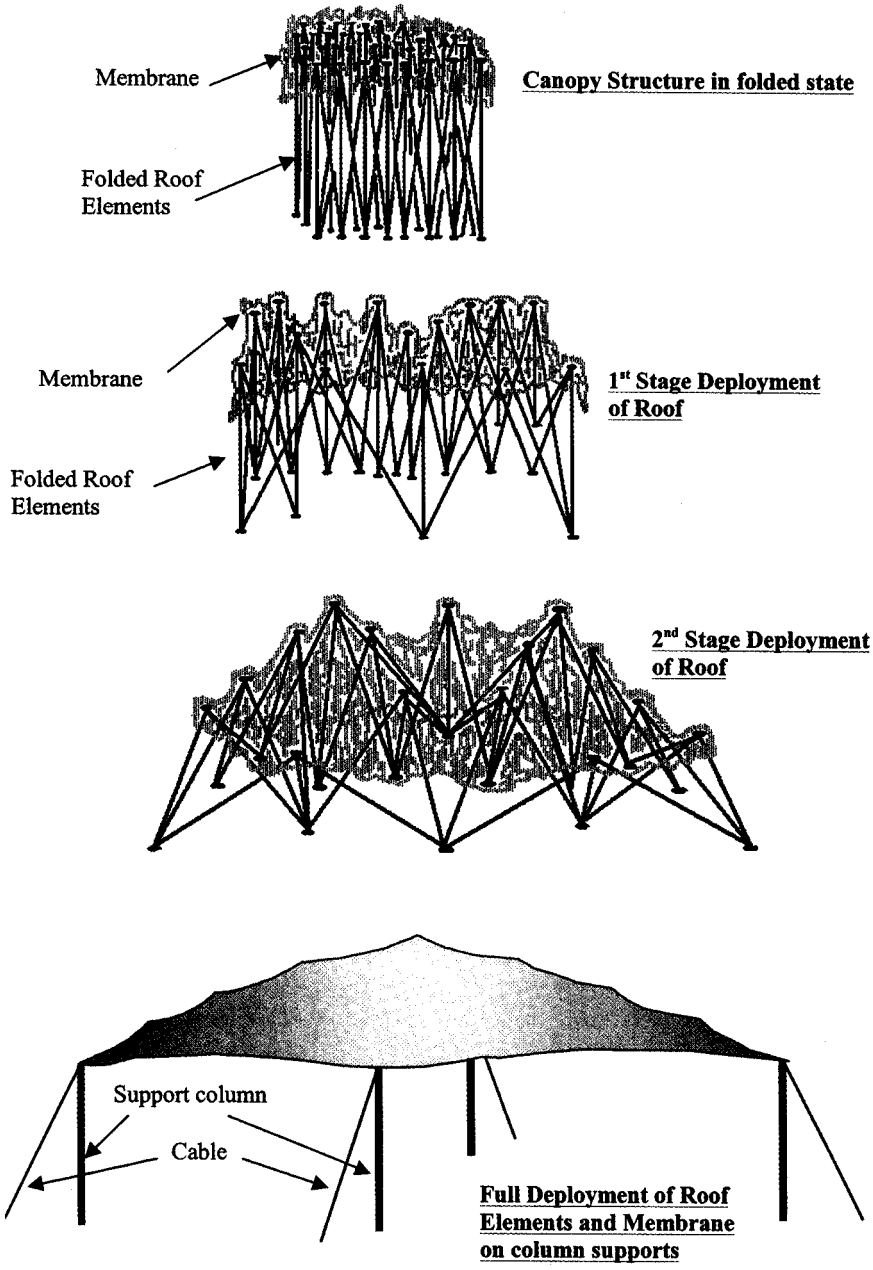

Fig. 1 Diagrammatic form of the different stages in the deployment of the 4.6 m by 4.6 m folding dome

typically less than 10 m in span, are often formed from tubular aluminium alloy members, joined at intervals with the membrane which is fixed to the skeletal framework after the erection of the structure, in much the same way as a frame tent is erected. A further class of system is being developed commercially, namely one that allows for the membrane to be deployed and stressed as the structure is being erected. It is the analysis and design of these particular structures that is the subject of this paper.

The dome structure under consideration is a prime example of a deployable structure constructed from an assembly of elements which is initially stored and transported as a tightly packed group of members and deployed *in-situ*, like an umbrella, into a dome structure, as shown in Fig. 1. One of the characteristics of a foldable structure is that it acts as a mechanism during deployment and usually requires the inclusion of additional elements in order to behave in a stable manner in the deployed position. However, this is not always true and, if the structure is carefully proportioned, usually by trial and error, it can snap through into a stable state under the application of a small force applied at a critical joint (Gantes 1997, You 1996).

The primary aim of this present study was to investigate the load-displacement response of these foldable domes under wind loading and assess the maximum wind speed that these structures could sustain in their deployed position. In addition, the failure characteristics of these structures were identified and recommendations made to enhance their stability and load carrying capability.

2. Dome configuration

The foldable dome structures considered were approximately 4.6 m by 4.6 m and were fabricated by Nomadic Spacestrut USA from a series of aluminium alloy 6061-T8 tubes, complying with British Standard 8118 Part 1 (1991), and thin steel cables. The fabric used to provide cover to the structure was a thin, opaque vinyl laminate membrane which was held in position at each of the structural node points. Fig. 1 shows, diagrammatically, the manner in which the structure is deployed, from the initial folded structure, through opening out to its final configuration. Fig. 2 shows a perspective view of the structure without the membrane attached. One type of basic structural unit used in foldable structures is a scissors-like element

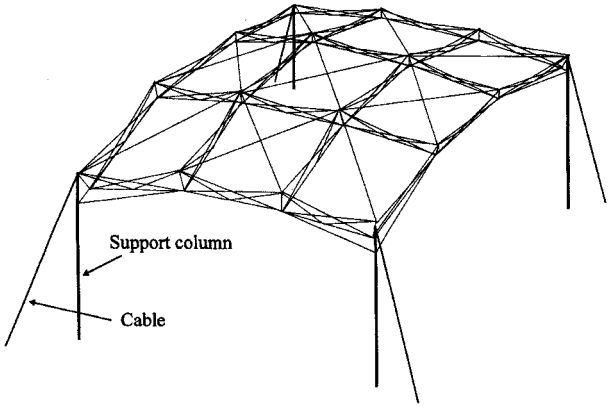

Fig. 2 Perspective view of the deployed structure

referred to as a duplet. A duplet consists of two tubes connected together, usually at their centre, by a pin and hinged at the four end points to the end nodes of other duplets. A connection or

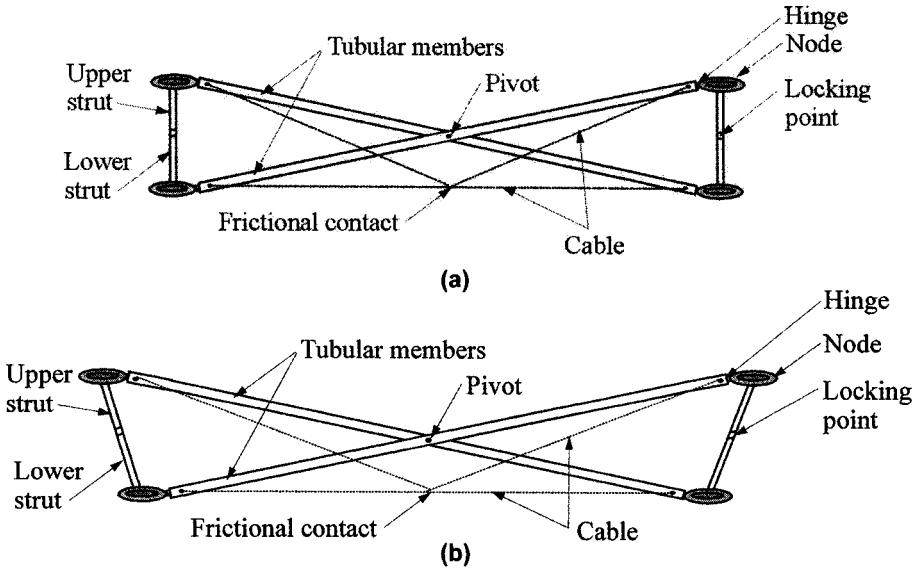

Fig. 3 (a) A rectangular duplet with K bracing and end nodes, (b) A trapezoidal duplet with K bracing and end nodes

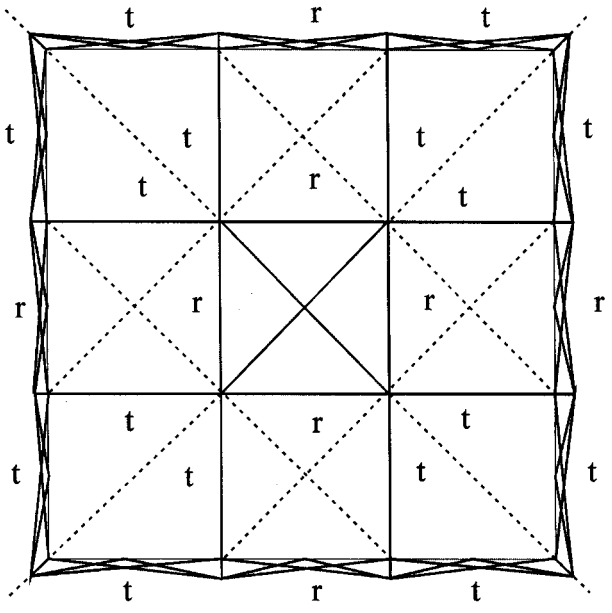

Fig. 4 The location of the rectangular and trapezoidal duplets in the folding dome structure

node in a foldable structure may connect together several cables and tubes while providing the kinematic freedom that each member requires. The domes considered consisted of two sizes of duplets, the internal duplets which were fabricated from 19 mm diameter tubes with a wall thickness of 0.92 mm and the external duplets which were fabricated from 25 mm diameter, 1.22 mm thick tubes. To brace the duplet elements, *K* shaped cable arrangements were used. In order to stabilise each duplet and consequently, the foldable configuration, two short struts, each projecting from an adjacent node, were locked together. Figs. 3a and 3b show the schematic representation of the two types of duplets and *K* cable bracing used in the structure, namely, rectangular and trapezoidal units. Fig. 4 shows the position in the dome of both types of duplets where the letters *t* and *r* are used to indicate the trapezoidal and rectangular units, respectively.

The joint used in the dome is required to connect together several tubes while providing the kinematic freedom that each member requires in order for the structure to fold and deploy correctly. Fig. 5 shows details of a typical member end and the node connector. The node is fabricated in two halves from high density polypropylene, both of which are joined together by four small screws. To allow the tubes to be joined to the nodes, small plastic end caps, together with a thin steel plate, were inserted into the aluminium tube ends and held in position by a steel dowel, as shown in Fig. 5. The thin steel plate protrudes from the member ends and fits into one of the slots located around the perimeter of each node. The steel plates were, in turn, located in the nodes using an open steel ring which is sandwiched inside the node and positioned before the two halves of the nodes are assembled together.

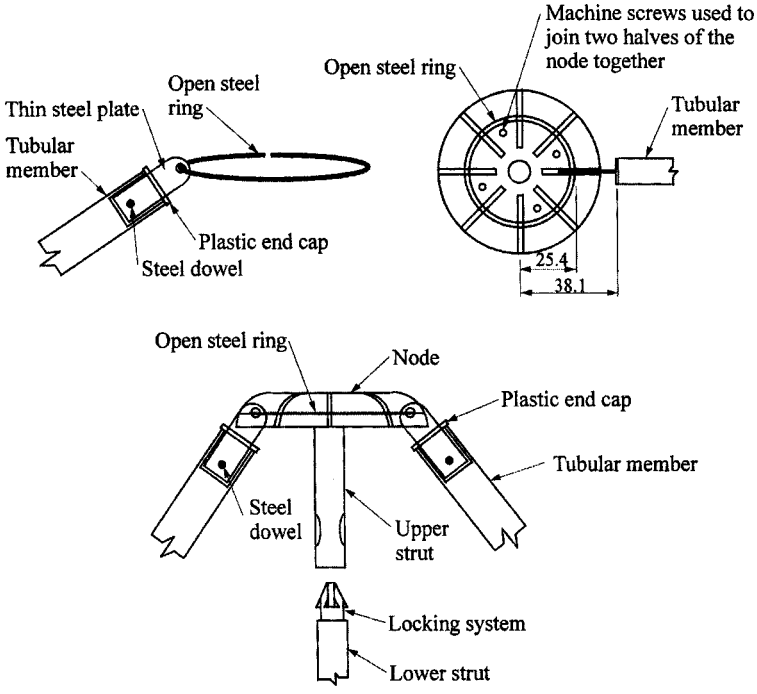

Fig. 5 Node and member end details

3. Wind tunnel analysis

3.1. Experimental investigation

The primary source of loading on lightweight canopy structures is that due to the action of the wind. However, it was noted by Cook (1990) that, prior to 1982, there had been no systematic studies of the wind loads on canopy structures. Subsequent research has encompassed measurements of wind pressures on mono-pitched and duo-pitched canopy structures at both full-scale, Robertson *et al.* (1985) and in wind tunnels using models, Gumley (1984), Robertson *et al.* (1986). However, these studies have been primarily concerned with the wind loads on open-sided agricultural canopy buildings of varying roof pitch and with different arrangements of internal blockage due to stored produce. Hence, the resulting design guidelines produced in BRE Digest 284 (1984), Robertson (1986) and BS 6399 (1995) are not directly applicable to the canopy structures considered in this paper. This is due to the fact that the full-scale structures considered by Robertson *et al.* (1985) had a ridge height of 7.2 m, whereas in the present study the canopy ridge (or crown) height was much smaller at only 2.4 m above the ground, thereby making the wind loads more strongly dependent on the local topography. In addition, the canopies studied and documented in the design guides relate only to mono or duo-pitched roof structures, whereas the canopy discussed here is pitched in all four orthogonal directions to give a single point crown rather than a ridge.

In order to provide wind loading on this type of structure, for implementation into the structural analysis programme, a wind tunnel analysis of the pressure distribution over the roof of a model of the 4.6 m × 4.6 m structure was performed. This work was carried out in one of the Department of Civil Engineering's boundary layer wind tunnels. This tunnel is of the open-circuit, blow-down type, constructed in a modular manner and is driven by a centrifugal fan through a wide-angle diffuser in which there are three sets of fine mesh screens. The air then passes through a settling chamber that contains a honeycomb and a further two mesh screens before passing through a 5:1 area-ratio contraction into the working section. This working section has dimensions of 1.675 m (height) × 1.372 m (width) × 9.0 m (length). The air then exhausts through a set of turning vanes into the laboratory.

Although the full-scale structure has a flexible membrane this membrane is stretched tight when the structure is fully deployed and as such, may be considered as a fixed surface under normal conditions. If this were not the situation then rapid deterioration in the material would occur. This being valid, a 1:10 scale model of the roof of the 4.6 m × 4.6 m folding dome was constructed from thin plywood giving an overall height to the tip of the central crown (H) of 240 mm. A total of 38 external pressure taps of 0.8 mm internal diameter were flush mounted in 1/8th of the surface area of the model. A further 4 pressure taps were located internally at equal locations on the underside of the crown of the canopy architecture. The model was constructed on a turntable that could be mounted in the floor of the wind tunnel such that, by revolving the model at discrete angles and utilising geometrical symmetry, the results from the 38 pressure taps provided the pressure distribution over the complete roof. The pressure tapings on the model were connected to a Scanivalve switch mechanism using short lengths of rubber tubing. The output (common) line of the Scanivalve switch allowed each tapping, in turn, to be connected to a Furness (UK) low-pressure differential transducer that measured the

difference between the pressure on the common line (the pressure tap) and the reference static pressure. The analogue voltage output from the transducer was amplified and then sampled by a personal computer.

The model was located in the wind tunnel at a distance of 7.5 m from the end of the contraction and its area blockage, compared to the wind tunnel cross-section, was less than 1%. Although it is good practice to simulate the local wind turbulence characteristics, occurring in the vicinity of the real structure, within the wind tunnel environment at the model location, it was considered that for this particular programme no attempt would be made. The reason for this was three-fold :

1. The full-scale structure was approximately 2.4 m in height and our knowledge of the turbulence intensity and scales within the lower 5 m of the atmospheric boundary layer is not well known, being somewhat dependent on local wind and topographic conditions.
2. Only the pressure distribution over the roof (without the sidewalls attached) was being considered and the maximum vertical extent of the model roof from eaves to crown was approximately 90 mm whilst the length and width were both 460 mm.
3. For the purpose of the structural analysis the general shape of the wind induced loading distribution was more important than the precise magnitudes when considering the stability of the structure.

Hence, a 20 mm high fence and a set of elliptical vortex generators were installed across the tunnel floor at the end of the contraction and a 2-D boundary layer allowed to develop naturally along the floor of the tunnel, up to the model position.

The mean velocity (U) and turbulence intensity (u^{1^2}) profiles associated with this boundary layer are shown in Fig. 6, giving a boundary layer thickness of approximately 287 mm. The corresponding displacement and momentum thicknesses at the model location were estimated to be 41 mm and 31 mm, respectively, with a freestream turbulence intensity of less than 0.20% and a turbulence level at the top of the model of 0.36%.

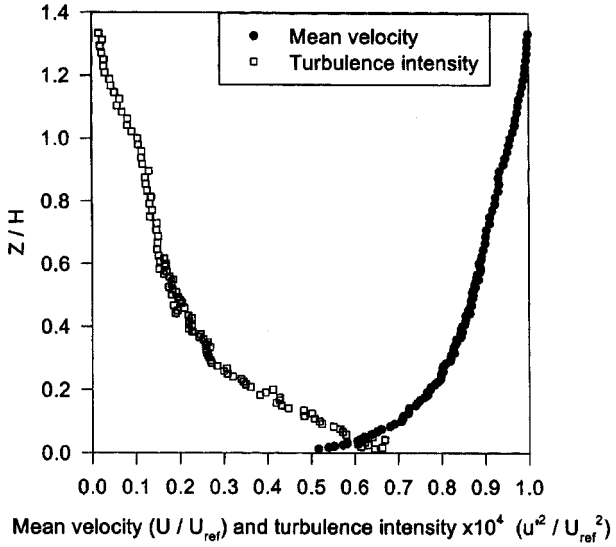

Fig. 6 Boundary layer profiles of mean velocity and turbulence intensity

Initially, a study of the static pressure variation at the model position was undertaken to establish the correct normalising parameters for the computation of the pressure coefficients. These static pressures were measured in the freestream, upwind of the model (Ps_1) and at the model position, in the absence of the model (Ps_2), over a range of freestream velocities (5 to 16 m/s) so that at each freestream velocity :

$$Ps_1 - Ps_2 = (\Delta Ps) \tag{1}$$

This correction to the static pressure was then applied in the main measurements programme to compute the non-dimensional pressure coefficient, $C_p=(P-P_s)/(0.5\,\rho U^2)$, where P and P_s are the surface pressure and the corrected freestream static pressure, respectively.

Two sets of measurements were carried out corresponding to two different model orientations. In configuration A the flow was perpendicular to one edge of the model whilst in configuration B, the model was at 45 degrees to the flow direction. The results of this analysis are shown in Figs. 7 and 8, respectively, where the pressure distribution is only shown over one half of the model for each of the configurations. These data were obtained at a reference dynamic pressure of 14 mm WG, equivalent to a freestream wind velocity (U_{ref}) of 15 m/s, giving a Reynolds number of 2.4×10^5 based on the overall canopy height. The transducer used for the pressure measurements was calibrated by a secondary standard to better than ±0.002 mm WG. This transducer had a very linear response such that it was possible to resolve pressures to within ±0.03 mm WG, thereby giving C_p values to within ±0.002.

It may be seen that for the perpendicular wind direction practically the entire upper surface of the roof experiences suction pressures. The peak coefficient value of -1.5, close to the

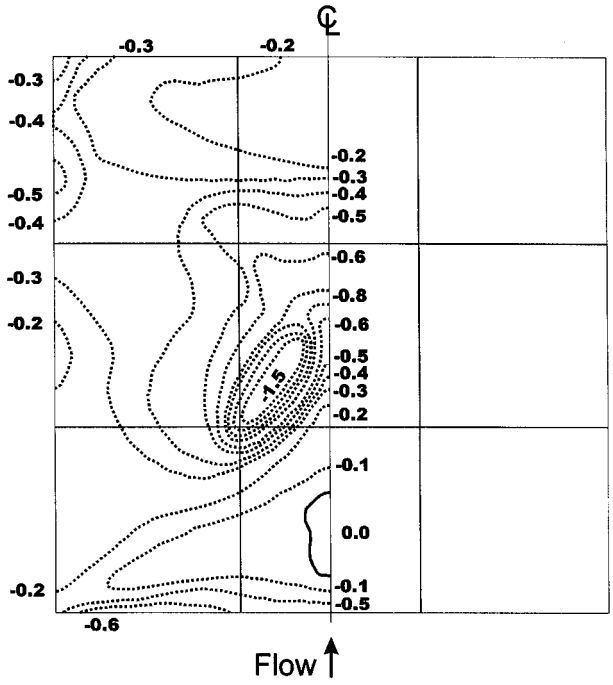

Fig. 7 Pressure coefficient distribution from the wind tunnel tests – (normal wind direction)

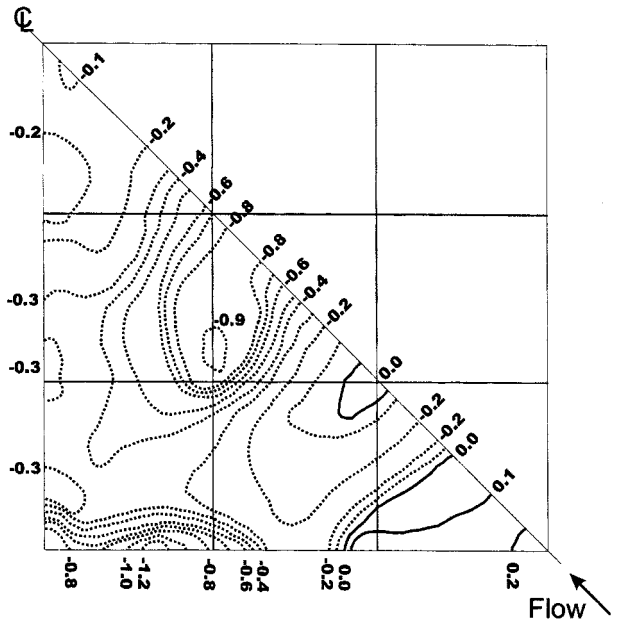

Fig. 8 Pressure coefficient distribution from the wind tunnel tests – (45 degree wind direction)

crown, is similar in magnitude to that found on duo-pitched canopy roofs, Robertson *et al.* (1985). With the wind at 45 degrees the positive pitch of the windward roof slopes means that small positive pressures occur near the corner of the windward eaves. Hence, the high suction pressures, associated with the 'delta-wing' type vortices which normally occur on flatter roofs for this wind direction, do not form on this pitched canopy structure. The local wind loadings were determined from these distributions by integrating over small discrete areas, taking into account the 'internal' pressures acting on the underside of the roof, and these loads were then incorporated into the structural analysis programme.

4. Structural appraisal

4.1. Experimental investigation

To allow the full non-linear characteristics of the dome to be modelled in the structural appraisal it was necessary to determine both the member and node load-displacement behaviour, through the linear response, up to failure. Several 19 mm and 25 mm diameter aluminium alloy tubes, both with and without their end nodes, were tested to failure in tension. In order to determine the ultimate capacity and the post-buckling, load-shedding behaviour, several tubular members, together with their end caps, were also tested to failure in compression. In addition, many tests to failure were undertaken to determine the ultimate capacity of both the cables and the cable clamp assemblies.

Fig. 9 shows typical tensile load-displacement responses obtained from both the 25 mm and 19 mm diameter aluminium alloy tubes tested with their end node assemblies. By comparing the responses shown in Fig. 9 with the behaviour of the tubes tested in tension

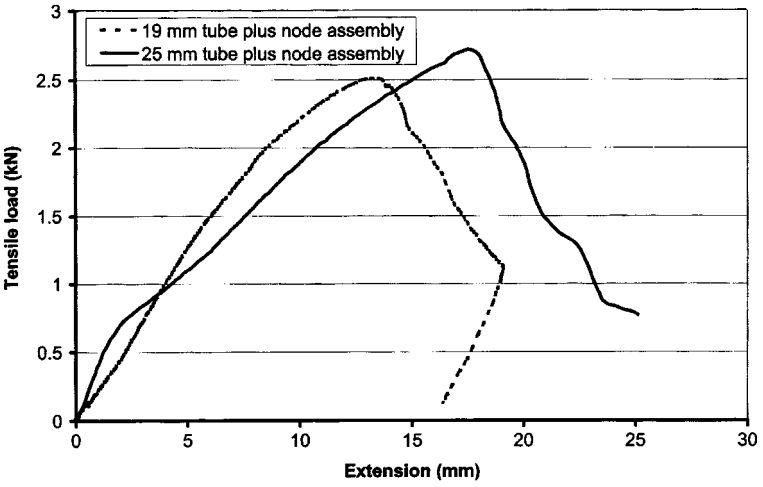

Fig. 9 Tensile load – displacement response for tubes plus node assemblies

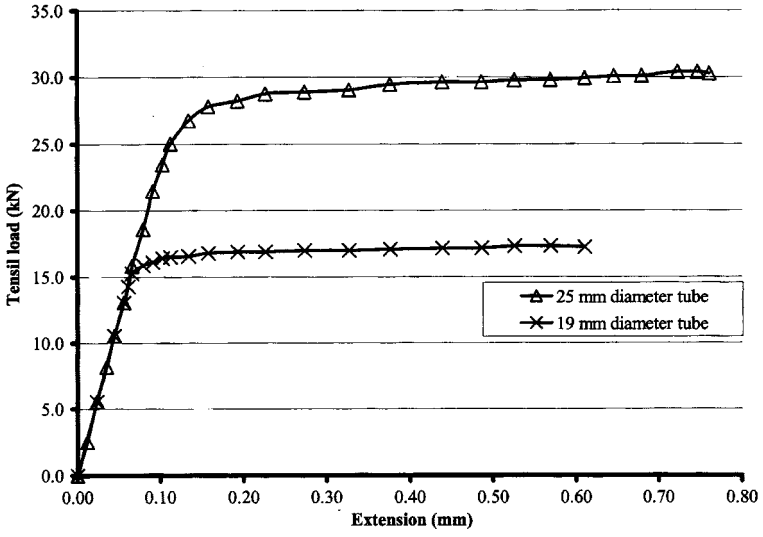

Fig. 10 Tensile load – displacement response for tubes without node assemblies

without their end nodes, shown in Fig. 10, it is evident that the presence of the end nodes dramatically reduces both the stiffness and strength of the tensile members. The tube and node assemblies tested in tension failed at one end node with the steel split ring inside the failure node elongating and finally pulling through the node side, forcing the two halves of the node apart. Fig. 11 gives typical load-displacement responses for both the 25 mm and 19 mm diameter tubes tested in compression with their two end caps. Comparing the behaviour shown in Fig. 11 with the theoretical compressive load-displacement response of both members without their end caps, as shown in Fig. 12, it is again apparent the presence of the end nodes reduces both the strength and stiffness of the compression members, as well as significantly altering the post buckling/failure characteristics.

Several 1.2 mm diameter steel cables plus their end clamps were also tested to failure in

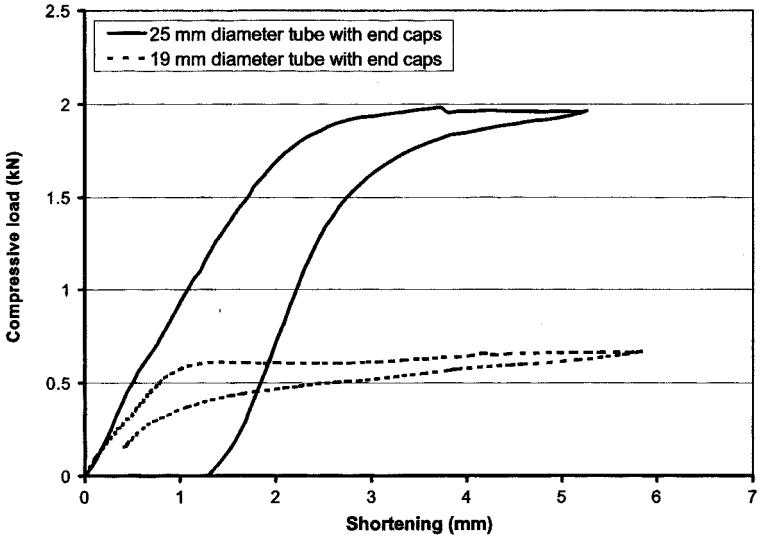

Fig. 11 Compression load – displacement response for tubes with end caps

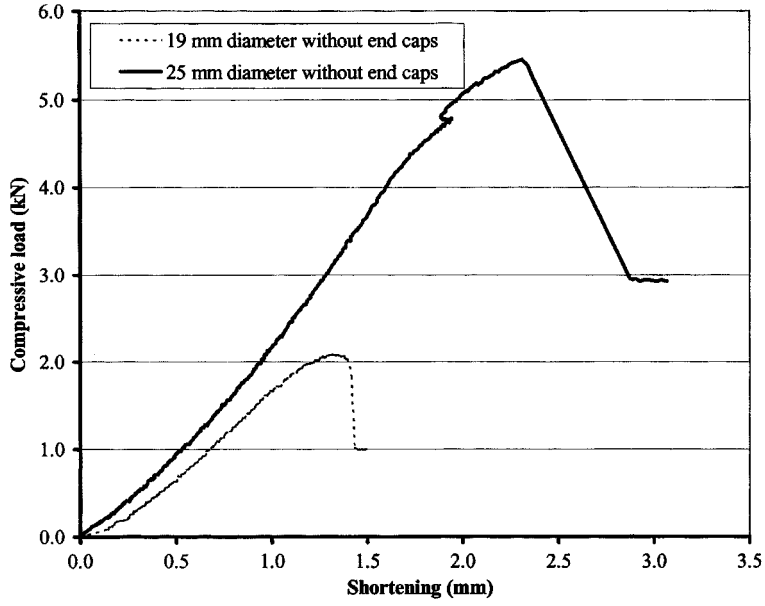

Fig. 12 Compression load – displacement response for tubes without end caps

tension, again to obtain the average values for Young's Modulus and ultimate tensile strength, which were necessary for the structural analysis. Some of the cables failed suddenly with the cable pulling out of one of the end clamps. However, for other specimens tested, a small amount of slip occurred at one end clamp, on several occasions, before final failure. Fig. 13 gives the load-displacement response obtained from two of the tensile tests and shows that, where intermediate slip did not occur, the cable exhibited an elastic response up to its sudden failure.

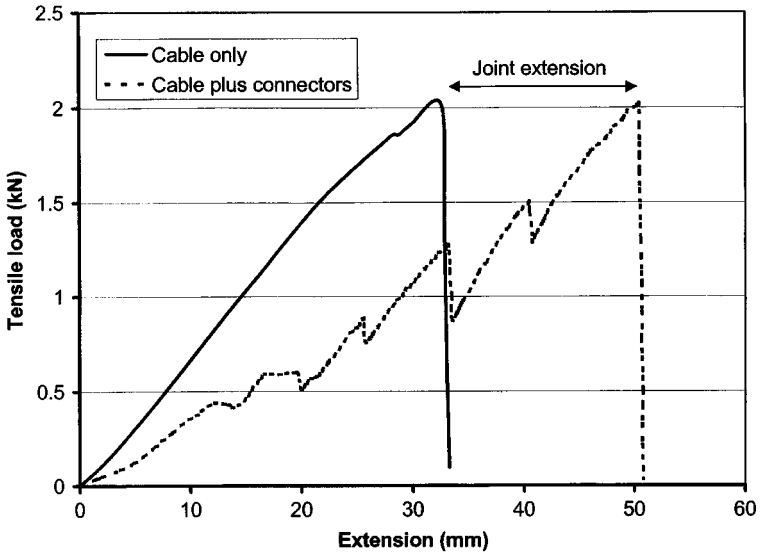

Fig. 13 Tensile load – displacement response for cables and cable plus connectors

4.2. Numerical modelling

The folding dome structure was modelled numerically using the finite element software ABAQUS (Hibbit *et al.* 1996). The initial dome configuration was generated using the in-house software Formian (Nooshin *et al.* 1994) which is a multi-facetted program ideally suited to the generation and processing of complex configurations. Fig. 14 gives the idealised load-displacement responses used in the numerical model to represent the real tensile and

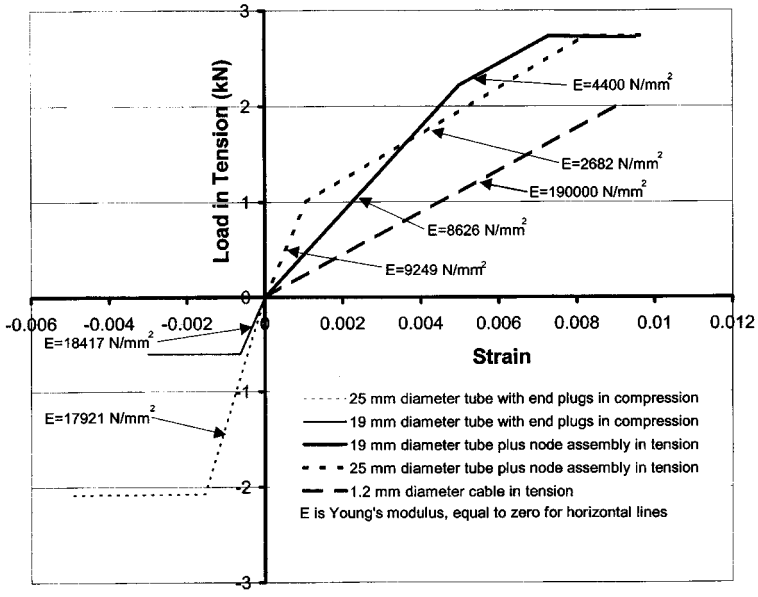

Fig. 14 Idealised load – displacement responses used in the analyses

compressive behaviour of both the 19 mm and 25 mm diameter tubes together with their end caps and end nodes. In addition, Fig. 14 also gives the idealised tensile load-displacement response used to model the real behaviour of the cable and clamp assemblies.

The folding dome structure required the use of 118 cable elements and 132 beam elements. The cable elements used in the analysis are two noded elements capable of only carrying axial tension. The beam elements are two noded 'non-linear beam general section' elements which are capable of accurately modelling real member behaviour. The elements take into consideration non-linear axial, shear, bending and torsional behaviour.

4.3. Non-linear analysis

In order to model the collapse behaviour of the dome structure a series of full non-linear analyses were undertaken. The analysis has taken into consideration large changes in geometry, node non-linearity and in addition, the spread of plasticity throughout member elements. Because the canopy is foldable it is also a structural mechanism which has to be prestressed in order to form a stable structure. As the data generation was undertaken using Formian this allowed the degree of member misfit to be determined before undertaking the structural analysis. In order to form both a stable structure and numerical model a small (10 kg) pre-stressing force was applied to the corner nodes to allow full deployment of the structure.

4.4. Modelling the scissors elements

The dome structure contained two sizes of scissors elements (duplets), the internal scissors fabricated from the 19 mm diameter aluminium alloy tubes and the external scissors made from the 25 mm diameter tubes. Scissors-type elements have been modelled previously, by other researchers, by adding non-linear rotational springs at the pivotal connections (Gantes *et al.* 1993, 1994). However, a modified approach was adopted for the structure under consideration where the scissors elements were split up into two tube elements which, in turn, were modelled as two connected beam elements (Fig. 15). By releasing the bending stiffness at each of the node ends of the tube elements the end nodes were forced to act as pinned. Where the two tubes crossed, at their central pivot points, a multi-point constraint facility was used to provide a pinned joint between the two central nodes. The multi-point constraint makes the displacements equal, but leaves the rotations, if they exist, independent of each other.

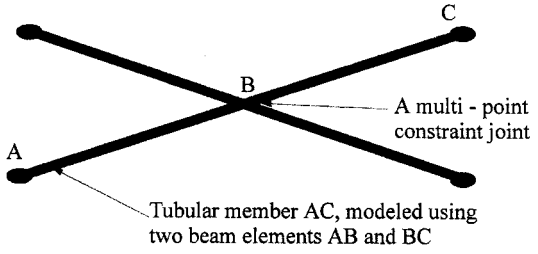

Fig. 15 Numerical modelling of scissors elements

4.5. Modelling the connection behaviour

The non-linear behaviour of the connections of the structure were modelled implicitly in ABAQUS using a 'JOINTC' element (Hibbit *et al.* 1996). This element consists of six adjacent springs, one allocated to each degree of freedom, which allow the true behaviour of the node, determined from tests, to be taken into consideration. This behaviour was incorporated into the behaviour of the scissors elements and allowed the comparison and validation of the mathematical model against the load-displacement response obtained from testing the members and nodes.

4.6. Modelling the membrane behaviour

In order to limit the total size of the numerical model, the membrane was modelled by using additional cable elements. This allows for the tensile strength of the membrane to be taken into consideration and will also model the compression behaviour of the membrane which loses stiffness when ripples or kinks occur.

4.7. Structural loading

The wind tunnel pressure distributions arising from the normal wind direction were converted into loading distributions for the structural analysis. The critical nodal loadings resulting from a 50 m/s wind speed for the 4.6 m square structure were then computed as a reference case. Because of the non-linear behaviour of the structure the loading has been applied incrementally, typically using over four hundred increments.

5. Numerical results

5.1. Model validation

In order to check the numerical finite element model, the 4.6 m square full size dome structure was assembled and loaded at certain specified nodes using known weights. The node displacements were then measured. This known loading regime was used in the analysis and all of the theoretical node deflections, emanating from the finite element analysis, were found to be within 10% of the actual measured deflections. Table 1 gives the values of the measured and theoretical node deflections. All of the theoretical deflections were slightly less than the measured deflections, indicating that the numerical model is slightly over-stiff compared to the real structure.

Table 1 The theoretical and measured node displacements obtained for the 4.6 m square dome structure

	Node Numbers				
	71	73	64	66	81
Measured displacements	-15.0 mm	-14.6 mm	-14.6 mm	-14.5 mm	-15.5 mm
Theoretical Displacement	-13.2 mm	-13.2 mm	-13.3 mm	-13.2 mm	-14.3 mm

5.2. Analysis A

The first numerical model for the 4.6 m square dome structure carefully followed the non-linear member and node behaviour obtained from the experimental tests. The structure failed at a total load of 0.12 times the reference loading value, equivalent to an approximate wind velocity of 17.3 m/sec (62 km/hr). Failure of the structure was assumed to occur with first member failure, corresponding to either the complete failure at the ultimate tensile strength for tension members, or at the individual buckling strength for the compression members.

The first elements to fail were the internal scissors members, numbers 49 and 50 (Fig. 16) which failed in compression primarily due to the poor behaviour of the end caps inserted into all of the aluminium alloy tubular members. The next most heavily stressed elements were two of the four corner steel tie down cable elements, numbers 27 and 28, which were supporting 62% of their ultimate tensile capacity. Table 2 gives details of the forces in other members within the structure at failure.

5.3. Analysis B

In order to assess the effect of various improvements on the folding domes the structures

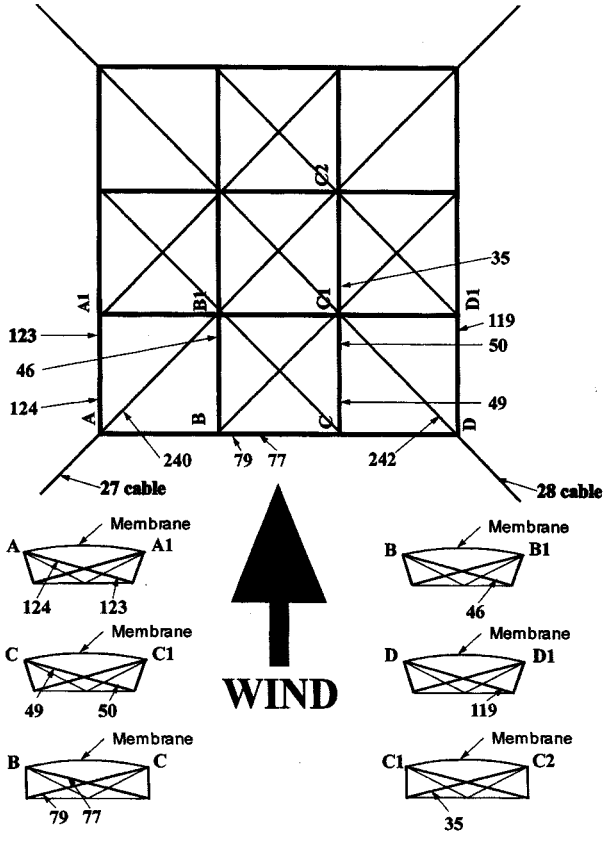

Fig. 16 Critical member numbers

Table 2 Failure loads and member capacity ratios for four different analyses

	ANALYSIS			
	A	**B**	**C**	**D**
Failure load. Percentage of loading applied for a 50 m/s reference wind	0.12	0.22	0.27	0.45
Equivalent wind speed at faiure (m/s)	17.3	23.4	26.0	33.5
First members to fail	Compression failure of internal scissors elements 49 and 50 (Fig. 16)	Tensile failure of corner tie down cables 27 and 28 (Fig. 16)	Compression failure of internal scissors elements 49 and 50 (Fig. 16)	Compression failure of external scissors elements 77 and 79 (Fig. 16)
Other most heavily stressed elements, together with the percentage of member ultimate capacity	Corner tie down cables 27 and 28 (62% of ultimate tensile capacity)	Internal scissors elements 49 and 50 (86% of compression capacity).	External scissors elements 119 and 123 (80% of compression capacity).	Internal scissors elements 35 and 50 (90% of compression capacity).
	External scissors elements 123 and 124 (60% of compression capacity).	External scissors elements 119 and 123 (65% of compression capacity).	Plan cable bracing 240 and 242 (65% of ultimate tensile capacity).	Plan cable bracing 240 and 242 (85% of ultimate tensile capacity).
		Plan cable bracing 240 and 242 (53% of ultimate tensile capacity).		Corner tie down cables 27 and 28 (80% of ultimate tensile capacity).

were re-analysed assuming improvements to both the connection behaviour and associated member end caps. This was achieved by preventing local deformation of all of the connection parts and also by using the theoretical behaviour of the aluminium alloy members obtained from a more detailed numerical appraisal of their behaviour as shown in Figs. 17a, b and c. With these improvements in connection and compression member behaviour the structure supported a total load of 0.22 times the reference loading value, equivalent to an approximate wind velocity of 23.4 m/sec (84 km/hr). Table 2 gives details of both the failed members and the forces in other parts of the structure at this load level.

5.4. Analysis C

In the third analysis undertaken for the structure the areas of all four of the corner steel tie down cables were increased by 100%, doubling the tensile capacity of these members. The

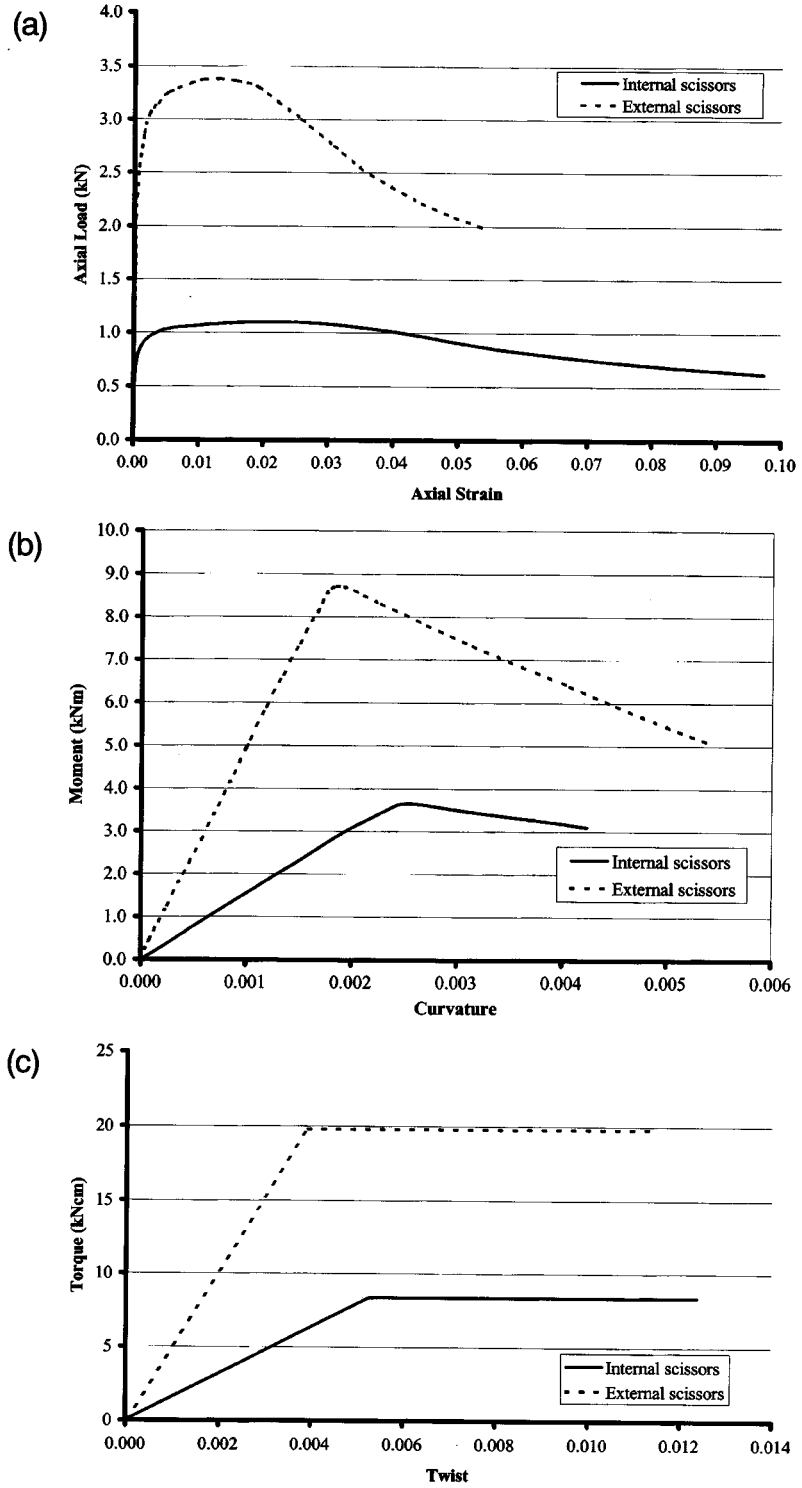

Fig. 17 (a) Theoretical axial load – strain relationship for scissors elements, (b) Theoretical moment – curvature relationship for scissors elements, (c) Theoretical torque – twist relationship for scissors elements

enhanced structure failed at a total load of 0.27 times the reference loading value, equivalent to an approximate wind velocity of 26 m/sec (93 km/hr), see Table 2.

5.5. Analysis D

For the final analysis of the folding dome the internal scissors elements, formed from the 19 mm diameter by 0.92 mm wall thickness aluminium alloy tubes, were replaced by 25 mm diameter by 1.22 mm wall thickness tubes. Also the diameter of the external scissors tubes was increased to 30.4 mm with a wall thickness of 1.2 mm. This resulted in an increase of 38% in the weight of aluminium and an overall increase of 25% in the total weight of the structure. This enhanced structure supported a total load of 0.45 times the reference loading value, equivalent to a approximate wind velocity of 33.5 m/sec (120 km/hr), see Table 2.

It should be noted that the analysis presented here has only included the case of the canopy without side walls. With three walls installed and the opening on the windward side, the positive internal pressures would significantly add to the overall lift force and hence increase the likely hood of failure at a lower wind speed.

6. Discussion

6.1. Wind loading

The C_p distribution has been used here to give the overall loading distributions for the structural analysis. Although the pressure coefficients were derived as time-averaged values, the failure wind speeds determined from the analysis should be considered as peak or upper-bound values. This is because this particular dome, which is a relatively small structure, will respond quite strongly to the variations in wind speed associated with turbulent gusts.

The wind tunnel investigation considered the wind forces acting only in two directions on the square dome. To improve the aerodynamic performance of the domes it may be beneficial to use inclined walls for the structures, or even semi-permeable vertical walls. In addition, if the membrane envelope were to include vents, this would minimise the positive internal pressures for the worst case of a windward wall opening thereby alleviating the overall loading on the structure.

6.2. Material tests

Although only a limited number of tests were undertaken to determine material properties and the behaviour of selected members and nodes, the average properties used in the numerical analysis were within $\pm 6\%$ of the maximum and minimum values obtained from the experimental investigation. No tests were undertaken to determine the tensile strength of the membrane which can play an important role in strengthening the structure. However, the tests undertaken have given a good insight into the behaviour of the domes and have highlighted areas of the structure which would benefit from strengthening. The behaviour of the test members and attached nodes, tested in tension, was governed solely by the node behaviour. Under a tensile load the inner steel ring inside the node distorted and opened up,

finally separating the two node halves. The node behaviour would be improved if, (a) the two ends of the steel ring were spot welded together, after the member ends were slotted on to the ring, or (b) if a 'key ring' were to be used which would not open up under a tensile load. In addition, if the four retaining screws holding the two halves of the node together were placed on the outside of the steel ring this would help to prevent node separation and contain the steel locating ring within the node (Fig. 5). Consideration could also be given to fabricating the node in a material which has a higher bearing strength, such as a glass filled polyester, which would reduce the tendency of the steel ring to crush the existing node material at points of high contact stress.

The tests undertaken on individual compression members and end caps indicated that the member response was governed by the compressibility and distortion of the end cap assemblies. Consideration should be given to determining ways of improving this end detail. It may be possible to fabricate a modified end using the existing stainless steel strips, together with aluminium alloy or glass filled polyester inserts, all of which may be assembled together and then bonded into the tubes.

6.3. Analytical investigations

From the numerical investigations undertaken using the finite element software ABAQUS it is evident that, if the dome nodes and member end caps could be enhanced, improved structural behaviour under wind loading could be obtained. The edge scissors elements proved to be heavily stressed, due to the high wind pressures at this location. In addition, increasing the strength of the four corner cable tie guys would prove beneficial for the structure.

It is important to note that the values of wind speed emanating from the numerical analysis assume that the dome structures are on level ground, upstream of and not adjacent to other structures.

7. Conclusions

From the analytical and experimental investigation undertaken, it is evident that the structural behaviour of the folding dome under consideration is very dependent on the load-displacement characteristics of both the structural joints and the member end caps. Enhancing the behaviour of the dome nodes will result in a direct improvement in the performance of the structure.

Consideration should also be given to ways of reducing the impact of wind loading on the structure and also ways of improving the aerodynamic profile of the dome. The latter could be achieved by fitting edge skirts or inclined walls to the dome, whilst semi-permeable membranes or vents in the membrane could be used to reduce internal and external pressure differences. It may also be possible to develop a 'smart' connection for attaching the cladding membrane to the structure. The design of this connection will allow the membrane to 'pop off' under high wind suctions, thereby avoiding damage to the structural framework.

Acknowledgements

This work has been supported by Mr Tom Wilson the Managing Director of Nomadic

Display, Louisburgh, Co. Mayo, Ireland, to whom the authors are indebted. The authors are also indebted to Dr Peter Disney and Dr Bahman Tahouri for help on the data generation and wind tunnel tests, respectively.

References

BRE (1984), "Wind loads on canopy roofs", *BRE Digest* 284, Building Research Establishment, Garston, UK.

BSI (1990), "BS 5950 Structural use of steelwork in building Part 1 : Code of practice for design in simple and continuous construction : hot rolled sections", London.

BSI (1991), "BS 8118 Structural use of aluminium Part 1 : Code of practice for design", British Standards Institution, London.

BSI (1995), "BS 6399 : Loading for buildings. Part 2 : Code of practice for wind loads", British Standards Institution, London.

Cook, N.J. (1990), "The designer's guide to wind loading of buildings and structures : Part 2-Static structures", Butterworths, London, p.222.

Gantes, C.J., Connor, J.J., Logcher, R.D. and Rosenfeld, Y. (1989), "Structural analysis and design of deployable structures", *Computers and Structures*, **32**(3-4), 661-669.

Gantes, C.J., Connor, J.J. and Logcher, R.D. (1993), "Simple friction model for scissor-type mobile structures", *J. of Eng. Mechanics*, **119**(3), 456-475.

Gantes, C.J., Connor, J.J. and Logcher, R.D., (1994), "Systematic design methodology for deployable structures", *Int. J. Space Structures*, **9**(2), 67-85.

Gantes, C.J., Giakoumakis, A. and Vousvounis, P., (1997), "Symbolic manipulation as a tool for design of deployable domes", *Computers and Structures*, **64**(1-4), 865-878.

Gumley, S.J., (1984), "A parametric study of extreme pressures for the static design of canopy structures", *J Wind Engineering and Industrial Aerodynamics*, **16**, 43-56.

Hibbit, Karlsson, and Sorensen (1996), "ABAQUS version 5.5", Providence, Rhode Island, USA.

Lewis, W.J. (1998), "Lighweight tension membranes an overview", *Proceedings of The Institution of Civil Engineers*, **126**(4), 171-181.

Nooshin, H. Disney, P. and Yamamoto, C. (1993), "Formian" Multi-Science Publishing, Brentwood, London.

Robertson, A.P., Hoxey, R.P. and Moran, P. (1985), "A full-scale study of wind loads on agricultural ridged canopy roof structures and proposals for design", *J Wind Engineering and Industrial Aerodynamics*, **21**, 167-205.

Robertson, A.P. and Moran, P. (1986), "Comparison of full-scale and wind tunnel measurements of wind loads on a free-standing canopy roof structure", *J Wind Engineering and Industrial Aerodynamics*, **23**, 113-125.

Robertson, A.P. (1986), "Design loads for ridged canopy roof structures", *J Wind Engineering and Industrial Aerodynamics*, **24**, 185-192.

You, Z. (1996), "Pantographic deployable conic structures", *Int. J. of Space Structures*, **11**(4), 363-370.

(Communicated by Chang-Koon Choi)